

Krzysztof MURAWSKI and Roman KOPER

Stability of Nonlinear Schrödinger Waves

Stabilność fal nieliniowego równania Schrödingera

1. INTRODUCTION

If the waves are thought to propagate in a certain medium and contribute to any significant physical phenomenon there, then that propagation needs to be confirmed by observation and theory — but preferably a combination of both. Of particular physical importance is then the question of stability: Is a given wave stable under perturbations, or will it evolve into something very different from its initial form? While linearizing to study the solution of the wave equation gives us information about the stability only for short times, as long as the linearization remains approximately valid. It tells us nothing about the long-time behaviour. So, the linear analysis is merely a first step in studying the stability of nonlinear waves.

There are many problems which are associated with the stability of nonlinear waves (e.g. [9]), and the literature on the subject is vast. We limit ourself to the presentation of some results on the stability of envelope waves which are described by nonlinear Schrödinger (NS) equations. (A recent derivation of the NS equation for magnetohydrodynamic waves in solar flux tubes has been presented by Zhelyazkov and Murawski [24]). In particular, Enns et al. [3] has discussed the following generalized NS equation

$$2iu_x + u_{tt} + uf(|u|^2) = 0, \quad (1.1)$$

where $f(|u|^2)$ is an arbitrary function. Possible higher-order nonlinear optical mechanisms leading to the nonlinearity $uf(|u|^2)$ are multiphoton res-

onances and light-induced phase transitions. The above equation possesses the solitary-wave solutions

$$u(t, x) = u_0(t - cx) \exp [i(kx/2 + ct)]. \quad (1.2)$$

It has been found by Enns et al. [3] that $dP/ds > 0$ guarantees stability against sufficiently small perturbations. Here, $s = k + c^2$ and the total power of a solitary wave is

$$P = \int_{-\infty}^{\infty} u_0^2 dt. \quad (1.3)$$

On the other hand, $dP/ds < 0$ guarantees unconditional instability. Moreover, solitary waves are robust solitons (they are stable even against large perturbations) if additionally the following conditions are satisfied: $f(|u|^2)/|u|^4 = 0(1)$ as $|u|^2 \rightarrow \infty$ and $f(|u|^2)$ is a non-negative and non-decreasing function for $|u|^2 > 0$. For example, the soliton of the NS equation (with $f(|u|^2) = |u|^2$) is robust in this sense.

A two-dimensional stability analysis of the nonlinear waves, solitons and shock-waves (or black solitons) solutions of the higher-order NS equation,

$$iu_t + \nabla^2 u + \alpha_1 |u|^{2n} u + \alpha_2 u = 0, \quad (1.4)$$

has been made by Murawski and Storer [18]. A special case of $n = 2$ has been taken into account to show that the shock-wave is stable with respect to two-dimensional perturbations but in contrast the soliton is unstable. The periodic waves have been found to be generally unstable with respect to the perpendicular perturbations. In the analysis $\alpha_2 \neq 0$ has been used and thus the calculations do not exclude an existence of the robustness of the soliton in the case of $\alpha_2 = 0$. See [3].

It has been shown by Wai et al. [22] that for the modified NS equation

$$iu_t + \frac{1}{2} u_{xx} + |u|^2 u = -i\Gamma u + i\beta u_{xxx} \quad (1.5)$$

there is a threshold for β above which the brothers (coupled solitons) of the NS equation can break up into three constituent solitons. Radiation that is excited after the first contraction of the brothers is then separated from the main peak creating two solitons. Menyuk [12] has found that below a certain initial amplitude threshold two-brother soliton breaks away creating two solitons which move in opposite directions relative to introduced coordinates. It suggests that the brother solitons are unstable with respect to disturbances which are introduced by the *r. h. s.* of equation (1.5).

In another case, the Infeld—Rowlands method [9] has been applied by Murawski and Koper [17] to study the linear stability of waves, propagation of which is governed by the exponential NS equation (Murawski [13]). This equation approaches the NS equation for small amplitude waves. The Infeld—Rowlands method has been used by Murawski et al. [19] to study stability properties of the two types of Zakharov equation waves. The Zakharov equation describes the evolution of the envelope of Langmuir waves with the nonlinearity introduced by a term involving the density fluctuation. The evolution of the density fluctuation is governed by the wave equation with the ponderomotive force exerted by the Langmuir wave.

Finally, the modulational instability of the NS equation can be utilized to produce a train of optical solitons which may be required whereby the encoding can be made (Hasegawa [4]). It is shown by Agrawal [1] that a new kind of modulational instability can occur when two copropagating electric fields interact through cross-phase modulation. Modulational stability of the modified NS equation has been studied by Parkes [20].

To the best of our knowledge there are no quantitative analytical results on the nonlinear stability of nonlinear waves. A basic approach to the stability problem relies on the linearization of perturbations (e.g. [9]). This paper addresses the problem of the nonlinear stability. It is confirmed numerically, that waves which satisfy the NS equation can exist in a real physical system as they are stable with respect to perturbations which are initially launched in the system.

The paper is organized as follows. The definition of the stability of nonlinear waves is presented in the next section of the paper. Stationary wave solutions of the NS equation are shown in the third section. Numerical solutions and results are given in the fourth and fifth parts of the paper. The transition of initial conditions into a train of solitons is shown in the Appendix.

2. DEFINITION OF STABILITY

There are few definitions of the stability of nonlinear waves. See e.g., [9] for a recent review of the literature. Here, by stability we mean the following. Assume we start with a solution $u(\xi, \tau)$ of the equation of motion $iu_\tau = X(u)$, where X is a differential operator, for example $X(u) = icu_\xi - \beta|u|^2u - \alpha u_{\xi\xi}$. ξ and τ are specified more precisely in the next section. Here, it is sufficient to relate ξ and τ with a space coordinate and time respectively. At $\tau = 0$ we add a small perturbation to the stationary envelope wave $u_0(\xi)$,

$$u(\xi, 0) = [u_0(\xi) + \delta u(\xi)] \exp(ia\xi), \quad (2.1)$$

and let this initial state evolve in time in accordance with the equation $iu_\tau = X(u)$. Now we ask, do $u(\xi, \tau)$ and $u_0(\xi)$ stay "close" to one another in some appropriate sense. If $u(\xi, \tau)$ grows apart in time or evolves to a different entity, the perturbation $\delta u(\xi)$ is unstable. A good example of the instability is provided by the Zakharov—Kuznetsov equation whose the perpendicularly disturbed flat (planar) solitary waves break up into cylindrical structures. See [15, 16] for the corresponding simulation of such processes. We specify the meaning of the stability by the following definition [11, 7]:

DEFINITION

An equilibrium solution $u_0(\xi)$ of the dynamical system $iu_\tau = X(u)$ is said to be stable in a *Liapunov* sense, if for every neighbourhood U of u_0 there is a neighbourhood V of u_0 such that trajectories $u(\xi, \tau)$ with $u(\xi, 0)$ initially in V never leave U , assuming well defined dynamics and a specified topology. In terms of a given norm $\|\cdot\|$, nonlinear stability means that for every $\epsilon > 0$ there is $\delta > 0$ such that $\rho_0 \equiv \|u(\xi, 0) - u_0(\xi)\| < \delta$ implies $\rho_\tau \equiv \|u(\xi, \tau) - u_0(\xi)\| < \epsilon$ for all τ .

There is no precise specification of the neighbourhoods U and V (or ϵ and δ). In fact both ϵ and δ are arbitrary but bounded quantities as the Liapunov stability concerns nonlinear perturbations which can be of arbitrary magnitude. For small amplitude perturbations, the results obtained by the Liapunov method should be similar to the results obtained by linear methods, for example by the Infeld—Rowlands method [9]. A solution can be stable with respect to one perturbation but unstable to the other.

We use the definition with a small modification. Namely, the Sobolev norm $\|u(\xi, \tau) - u_0(\xi)\|$ specified by

$$\rho_0 \equiv \|f\|^2 = \int_{-\infty}^{\infty} \left(|f|^2 + \left| \frac{\partial f}{\partial \xi} \right|^2 \right) d\xi, \quad (2.2)$$

will be used for the calculation of a distance between the solution $u(\xi, \tau)$ and the 'closest' stationary solution $u_0(\xi)$. By that way, for $\tau = 0$ we use expression (2.2) whereas for arbitrary time τ , we use

$$\rho_\tau \equiv \inf_{s, \tau^*} \|u(\xi, \tau) - u_0(\xi - s) \exp \{i[a(\xi - s) + b(\tau - \tau^*)]\}\|, \quad (2.3)$$

where $\|\cdot\|$ denotes the Sobolev norm and \inf_{s, τ^*} denotes the infimum with respect to s and τ^* . The 'closest' (to $u(\xi, \tau)$) solution is thus found by

a translation in time τ^* and space s . See as well [2] and [10] for a more detailed discussion.

3. STATIONARY SOLUTIONS

In this part of the paper we discuss various solutions of the NS equation

$$iu_t + \beta|u|^2u + \alpha u_{xx} = 0. \quad (3.1)$$

In coordinates of the moving frame ξ, τ (which follows the wave with its group velocity c)

$$\xi = x - ct, \quad \tau = t, \quad (3.2)$$

it can be rewritten as follows:

$$i(u_\tau - cu_\xi) + \alpha u_{\xi\xi} + \beta|u|^2u = 0. \quad (3.3)$$

We look now for the stationary solutions of the form

$$u(\xi, \tau) = u_0(\xi) \exp[i(c\xi/2\alpha + b\tau)], \quad (3.4)$$

where b is an arbitrary constant. This solution represents a slowly varying envelope $u_0(\xi)$ and the fast oscillations which are represented by the exponential term. Substitution of (3.4) into equation (3.3) leads to

$$\alpha u_0 \xi + (\beta u_0^2 + p)u_0 = 0, \quad (3.5)$$

where we introduced

$$p \equiv \frac{c^2}{4\alpha} - b. \quad (3.6)$$

Upon integration of this equation we get

$$u_0^2 = -\frac{\beta}{2\alpha}u_0^4 - \frac{p}{\alpha}u_0^2 + l \equiv Y(u_0), \quad (3.7)$$

where l is an integration constant.

Equation (3.7) describes the stationary solutions of the NS equation (3.1). Defining

$$l_{min,max} \equiv \min, \max \left\{ 0, -\frac{p^2}{2\alpha\beta} \right\} \quad (3.8)$$

we can distinguish the following families of solutions.

(i) The *soliton* family contains both for $l_{min} < l < l_{max}$ and $l > l_{max}$ periodic waves (Fig. 1). We call them *R* and *S* waves, respectively. $l = l_{max}$

corresponds to the soliton. This family exists under the condition $\alpha\beta > 0$ and $p\beta < 0$. The soliton solution (for $\alpha = 1$ and the original coordinates x, t) is given by the equation

$$u_0(x, t) = A \operatorname{sech} \left[\sqrt{\frac{\beta}{2}} A(x - Bt - s) \right] \exp[iB(x - ct)/2]. \quad (3.9)$$

where A and B are arbitrary constants, $c < \frac{B}{2}$, and s is a shift parameter. The R and S periodic waves are given by the corresponding equations

$$u_0^2 = a_2^2 - (a_2^2 - a_1^2) \operatorname{sn}^2 \left[\pm a_2 \sqrt{\frac{\beta}{2\alpha}} \xi |m_1 \right], \quad (3.10)$$

$$u_0^2 = a_1^2 \left\{ 1 - \operatorname{sn}^2 \left[\pm \sqrt{\frac{\beta(a_1^2 + a_2^2)}{2\alpha}} \xi |m_2 \right] \right\}, \quad (3.11)$$

respectively. In the above formulae a_1 and a_2 are the moduli of roots of the equation $Y(u_0) = 0$ such that $a_1 < a_2$; $Y = -\frac{\beta}{2\alpha}(u_0^2 - a_1^2)(u_0^2 - a_2^2)$ and $Y = -\frac{\beta}{2\alpha}(u_0^2 - a_1^2)(u_0^2 + a_2^2)$ for equation (3.10) and (3.11), respectively. $\operatorname{sn}(z|m)$ is a Jacobian elliptic sine function of the arguments z and m . $m_1 = 1 - a_1^2/a_2^2$, $m_2 = a_1^2/(a_1^2 + a_2^2)$.

(ii) The *periodic wave* family contains only periodic waves given by the formula (3.11). This family exists under the condition of $\alpha\beta > 0$ and $p\beta > 0$. One such wave is called T . See Figure 2 for the corresponding phase diagrams.

(iii) The *shock wave* family contains for $l_{\min} < l < l_{\max}$ periodic waves. We call them U and they are given by the expression

$$u_0 = \pm a_1 \operatorname{sn} \left[\pm \sqrt{\frac{-\beta a_2^2}{2\alpha}} \xi |m \right] \quad (3.12)$$

with $m = a_1^2/a_2^2$. For $l = l_{\max}$ there is a shock wave (or black soliton) solution which is expressed by

$$u_0 = \sqrt{-\frac{p}{\beta}} \tanh \left[\pm \sqrt{\frac{|p|}{2|\alpha|}} \xi \right]. \quad (3.13)$$

This family exists under the condition $\alpha\beta < 0$ and $p\beta < 0$. See Figure 3 for the phase curve.

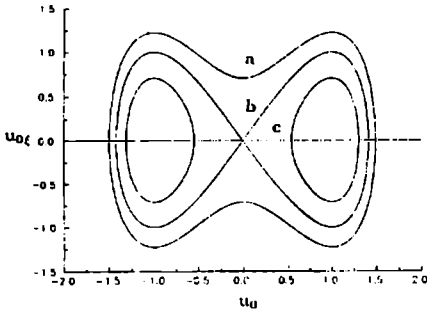


Fig. 1. Phase diagrams for the NS equation with $\alpha = 1$, $\beta = 2$, $a = -2$: curve a, the periodic wave S ; curve b, the bright soliton; curve c, the periodic wave R

Ryc. 1. Wykresy fazowe dla nieliniowego równania Schrödingera z $\alpha = 1$, $\beta = 2$, $a = -2$: krzywa a odpowiada fali okresowej S ; krzywa b odpowiada jasnemu solitonowi; krzywa c odpowiada fali okresowej R

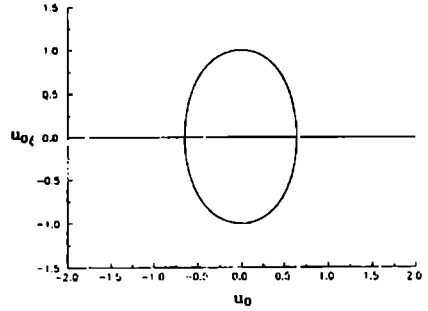


Fig. 2. Phase diagrams for the NS equation with $\alpha = 1$, $\beta = 2$, $a = 2$ corresponding to the periodic wave T

Ryc. 2. Wykresy fazowe dla nieliniowego równania Schrödingera $\alpha = 1$, $\beta = 2$, $a = 2$. Wykresy te odpowiadają fali okresowej T

It has been shown by Hasegawa [5] that the NS equation possesses also the dark soliton solution which is given by (written here for $\alpha = -\frac{1}{2}$ and $\beta = 1$)

$$u(x, t) = \sqrt{A_s[1 - A_a^2 \operatorname{sech}^2(\sqrt{A_s} a_a x)]} \exp[i\phi(x, t)], \quad (3.14a)$$

$$\begin{aligned} \phi(x, t) = & \sqrt{A_s(1 - A_a^2)}x + \tan^{-1}\left[\frac{A_a}{\sqrt{1 - A_a^2}}\right] \times \\ & \times \tanh(\sqrt{A_s} A_a x) - \frac{1}{2}A_s(3 - A_a^2)t, \quad |A_a| \leq 1. \end{aligned} \quad (3.14b)$$

For $|A_a| < 1$ we obtain the so-called gray solitons whereas for $|A_a| = 1$ the black soliton (3.13) appears. See as well [6] and [21].

It has been found by Infield and Rowlands [8] that the bright soliton (3.9) is linearly stable with respect to small amplitude long-wavelength perturbations. Similarly, the S and U periodic waves are stable with respect to the same kind of perturbations. The R wave is found to be unstable. From the corresponding discussion for the nonlinear exponential Schrödinger waves [17] we suppose that the T wave is stable. Nothing is known so far about the stability of the dark soliton solutions (3.14).

4. NUMERICAL SOLUTIONS

The numerical codes utilize the leap-frog method in an integration with respect to time. The nonlinear terms are integrated in a configuration space. The second derivative with respect to the space coordinate x is calculated by transforming $u(x, t)$ back and forth between real and Fourier space using the fast Fourier transformations. Similar method has been used by Murawski [15] for solving three-dimensional Zakharov—Kuznetsov equation.

The NS equation is discretized as follows:

$$u_j^{n+1} = u_j^{n-1} + 2i\Delta t \left[\alpha F^{-1}(-m^2 F u_j^n) + \beta |u_j^n|^2 u_j^n \right] \quad (4.1)$$

with $u_j^n = u(j\Delta x, n\Delta t)$, $j, n = 0, 1, \dots$. F and F^{-1} are the Fourier and inverse Fourier operators, respectively. For a similar discretization of the exponential NS equation see [13, 14].

Equation (4.1) is numerically solved with the initial condition

$$u(\xi, 0) = [u_0(\xi) + A_d \sin(k_d \xi)] \exp[ic\xi/2\alpha], \quad (4.2)$$

where A_d and k_d are the amplitude and wave number of the disturbances. For this purpose the code SH.FOR has been written. Another code PER.FOR finds Jacobian elliptic functions for solutions (3.10)–(3.12) representing periodic waves.

Standard numerical tests have been performed by doubling a number of Fourier modes, reducing time step and increasing a simulation region until no significant changes appear. Additionally, the numerical results have been verified by a calculation of the energy

$$\int_{-\infty}^{\infty} |u|^2 d\xi \quad (4.3)$$

as a conserved quantity. It has been checked that this quantity was approximately constant with a numerical error which was less than 2%.

5. NUMERICAL RESULTS

One of codes, LIAP.FOR, has been written to study stability of stationary waves in the Liapunov sense. Because this code is computer time consuming we have run the code for the R wave which, according to the linear analysis (Infeld and Rowlands, [8]), is unstable. Obtained results may be found in Figure 4. Starting with a disturbance which gave us Sobolev norm (2.2) equal to about 0.04 the norm ρ_t jumped in next time steps to

about 5 to oscillate finally between these two values, but with a tendency of growing. As the norm grows in time the R wave is unstable. Because of very expensive code this problem is left for future computer studies and the problem has been reduced to the initial-value one for the NS equation.

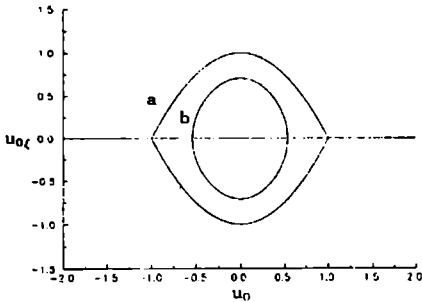


Fig. 3. Phase diagrams for the NS equation with $\alpha = 1$, $\beta = -2$, $a = 2$: curve a, the shock wave (or black soliton); curve b, the periodic wave U

Ryc. 3. Wykresy fazowe dla nieliniowego równania Schrödingera $\alpha = 1$, $\beta = -2$, $a = 2$: krzywa a odpowiada fali szokowej (tzw. czarnemu solitonowi); krzywa b odpowiada fali okresowej U

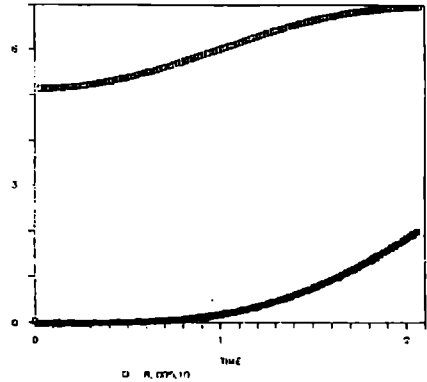


Fig. 4. The Sobolev norm as a function of the time t for the R wave under the initial perturbations with $A_d = 0.005$ and $k_d = 10$

Ryc. 4. Norma Sobolewa jako funkcja czasu t . Rysunek odpowiada fali R i zaburzeniu początkowemu o amplitudzie $A = 0,005$ i wektorze falowym $k = 10$

According to our expectation the bright soliton (3.9) with an amplitude $A = 1$ has been found to be stable with respect to disturbances given by (4.2). We have run the following cases: a) $A_d = 0.05$, $k_d = 0.05$, b) $A_d = 0.05$, $k_d = 1$, c) $A_d = 0.2$, $k_d = 0.05$, d) $A_d = 0.2$, $k_d = 1$. The soliton behaved very robust to these perturbations.

To test the stability of the periodic waves we have chosen $c = 0$ because of Galilean invariance of the NS equation. Additionally, we fixed the wave vector $k_d = 10$.

1) R wave

We have chosen a representative wave for $l = (l_{max} + l_{min})/2$. This wave is stable to numerical noise until time $t = 100$. Weak instabilities have been noticed for $A_d = 0.005$. The hump at $x = 0$ has grown considerably at $t = 100$ with a comparison to the neighbouring humps (Fig. 5).

2) S wave

We have chosen a representative wave with $l = l_{max} + |l_{max} + l_{min}|/2$. This wave has been found to be stable both to numerical noise and the disturbances with $A_d = 0.005$. For $A_d = 0.05$, the disturbances are clearly visible at $t = 0$ (Fig. 6), but until time $t = 100$ they do not cause any dramatic changes of the wave form which at $t = 60$ became even smoother.

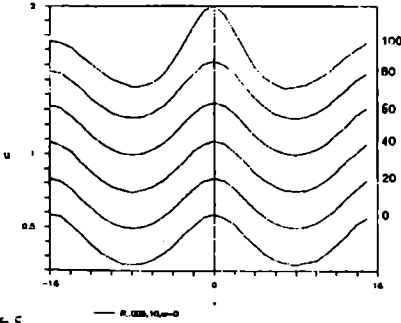


Fig. 5. Panoramic view of the periodic wave R under the initial perturbations with $A_d = 0.005$ and $k_d = 10$. Note that at $t = 100$ the shape of the wave is considerably deformed. This is an evidence of the instability

Ryc. 5. Panoramiczny widok na falę R , którą zaburzone falą sinusoidalną o amplitudzie $A = 0,005$ i wektorze falowym $k = 10$. Warto zauważyć, że w chwili czasu $t = 100$ fala ulega znacznej deformacji, co jest dowodem pojawienia się niestabilności

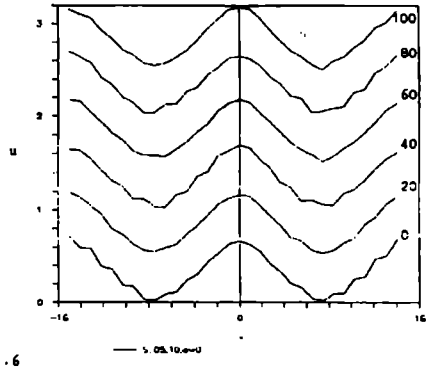


Fig. 6. Panoramic view of the periodic wave S under the initial perturbations with $A_d = 0.05$ and $k_d = 10$. This wave is stable

Ryc. 6. Panoramiczny widok na falę R , którą zaburzone falą sinusoidalną o amplitudzie $A = 0,05$ i wektorze falowym $k = 10$. Fala ta jest stabilna

3) T wave

We have chosen a wave which corresponds to $l = 0.01$. The wave has been found to be stable both to numerical noise and to the disturbances with $A_d = 0.005$. Note that the amplitude of perturbations $A_d = 0.05$ consists almost 10% of an amplitude of the wave, which much deformed at $t = 0$ looks quite smooth at $t = 100$ (Fig. 7).

4) U wave

We have chosen a representative wave with $l = (l_{max} + l_{min})/2$. This wave is stable to the perturbations with $A_d = 0.005$ and $A_d = 0.05$ (Fig. 8).

Figure 9 and 10 present typical results of the computation for the stability of the gray solitons which are described by (3.14). We have chosen $A_s = 1$, $A_d = 0.8$. It has been found that these gray solitons are stable to numerical noise. The code has been run until time $t = 25$ and both the shape and an amplitude of the soliton oscillated slightly around their undisturbed values. Moreover, this soliton is stable both with respect to long wave (Fig. 9) and short wave (Fig. 10) perturbations. We have fixed the amplitude of the disturbances $A_d = 0.04$, which consists 10% of the soliton amplitude.

Summing up, both the gray and bright solitons are quite robust to the disturbances we have used. For the periodic waves, the R wave is unstable to the perturbations. The results for the bright soliton and the periodic waves agree with the linear theory presented by Infeld and Rowlands [8]. Additionally, the obtained results provide a new insight into the stability of the gray solitons.

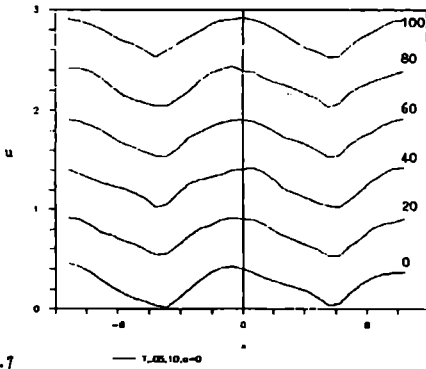


Fig. 7. As for Fig. 6 but here for the T periodic wave
 Ryc. 7. Tak, jak dla Ryc. 6, ale dla fali okresowej typu T

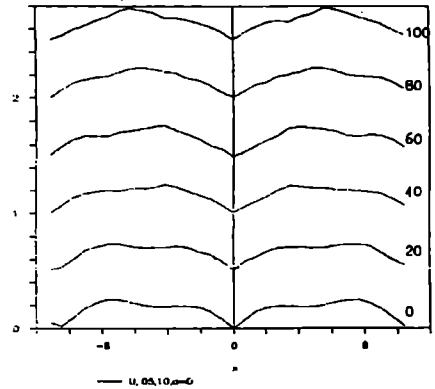


Fig. 8. As for Fig. 6 but here for the U periodic wave
 Ryc. 8. Tak, jak dla Ryc. 6, ale dla fali okresowej typu U

6. THE APPENDIX

In this Appendix, we solve numerically the NS equation for the following classes of perturbations

$$u(x, t = 0) = 0.1 \operatorname{sech}^2 x, \tag{A.1}$$

$$u(x, t = 0) = 0.1 - 0.05 \operatorname{sech}^2 x. \tag{A.2}$$

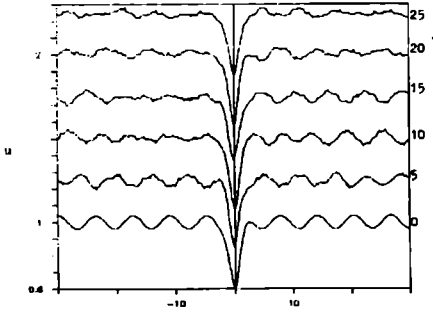


Fig. 9

Fig. 9. Panoramic view of the soliton solution with $A_s = 1$ and $A_a = 0.8$ under the initial perturbations with $A_d = 0.04$ (10% of the soliton amplitude) and $k_d = 1$. The soliton survived these perturbations

Ryc. 9. Panoramiczny widok na soliton o parametrach $A = 1$ i $A = 0,8$. Soliton ten zaburzone fali sinusoidalną o amplitudzie $A = 0,04$ (10% amplitudy solitonu) i wektorze falowym $k = 1$. Soliton ten przetrwał to zaburzenie

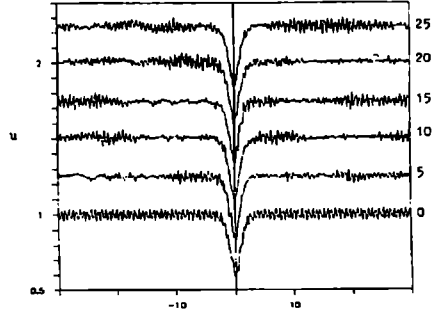


Fig. 10. As for Fig. 9 but here $k_d = 10$
Ryc. 10. Tak, jak dla Ryc. 9, ale dla $k = 10$

Figures 11(b) and 12(b) are plotted for the initial conditions given by (A.1). Figures 11(a) and 12(a) correspond to perturbation (A.2). Figure 11 is made for $\alpha = -0.01$ and $\beta = 27.55$. Figure 12 is obtained for $\alpha = 0.04$ and $\beta = 52.01$. Such values of α and β correspond to MHD waves which propagate in the solar chromosphere [24].

We discuss first the case of a negative α . It is known that the NS equation with $\alpha\beta < 0$ possesses the dark soliton solution. (See Eq. (3.14)). Figure 11(a) presents a temporal evolution of the initial perturbation (A.2) which splits soon into two almost identical pulses, propagating in opposite directions. They are well seen at $t = 40$. At this moment every large pulse pushes off a small pulse. The large and small pulses are well separated at $t = 80$. The initial perturbation evolves into the trail of the dark solitons.

Whereas the initial condition (A.1) splits up into the dark solitons, the perturbation (A.2) diffuses in time, reducing its amplitude and broadening its shape (Fig. 11(b)). At $t = 40$ the perturbation is about twice wider than initially. As the case of $\alpha\beta < 0$ does not allow bright solitons, the perturbation transforms into the periodic wave with its dimensionless wavelength $\lambda \simeq 40$. This periodic wave emerges at $t = 80$.

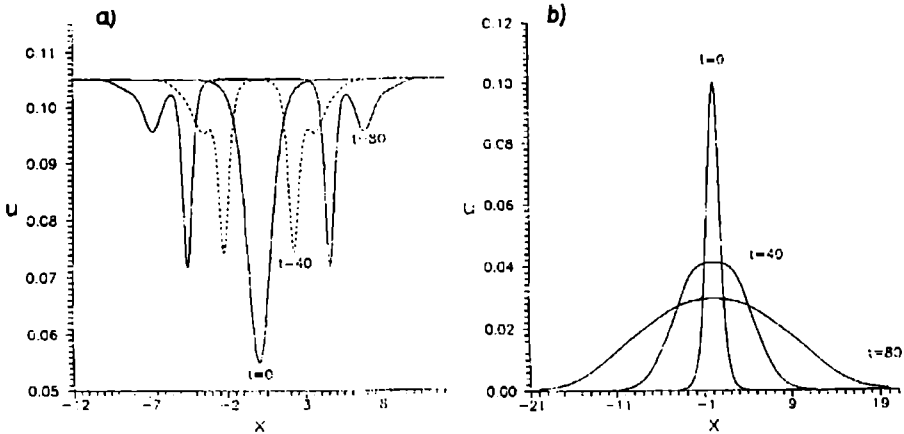


Fig. 11. Panoramic view of modulation envelope for the NS equation with $\alpha = -0.01$ and $\beta = -27$. The initial conditions are: (a) $u(x, t = 0) = 0.1 - 0.05 \operatorname{sech}^2 x$; (b) $u(x, t = 0) = 0.1 \operatorname{sech}^2 x$. Note the trail of the dark solitons at $t = 80$ in (a)

Ryc. 11. Panoramiczny widok na obwiednię fali będącej rozwiązaniem nieliniowego równania Schrödingera z $\alpha = -0,01$ i $\beta = -27$. Warunki początkowe to: (a) $u(x, t=0) = 0,1 - 0,05 \operatorname{sech}^2 x$; (b) $u(x, t = 0) = 0,1 \operatorname{sech}^2 x$. Zauważ ciąg ciemnych solitonów w chwili czasu $t = 80$ w (a)

Finally, we discuss the case of positive α . Figure 12(a) presents typical results of computation for the initial condition (A.2). The case of $\alpha\beta > 0$ does not possess the dark solitons but the periodic waves (3.10) and (3.11) instead. The initial condition leads to a trail of periodic-like oscillations which propagate off the point $t = 0$.

An interesting case occurs for the initial perturbation (A.1). Now, at $t = 5$ we have a dressed bright soliton (Figure 12(b)). The dressing is by two small humps which are located at the central pulse. This dressed soliton has a higher amplitude than the initial one. But it is narrower as fields under each curve are the same. At $t \simeq 15$ the dressed soliton reduces its amplitude and it is similar in its shape to the initial perturbation. Then, it grows again. At $t \simeq 20$ it is reminiscent of the perturbation at $t = 5$. As this process repeats in time we call it *recurrence phenomenon*. The recurrence phenomenon has been observed for sinusoidal perturbations in the case of the NS equation [5] and in the case of the exponential NS equation [14].

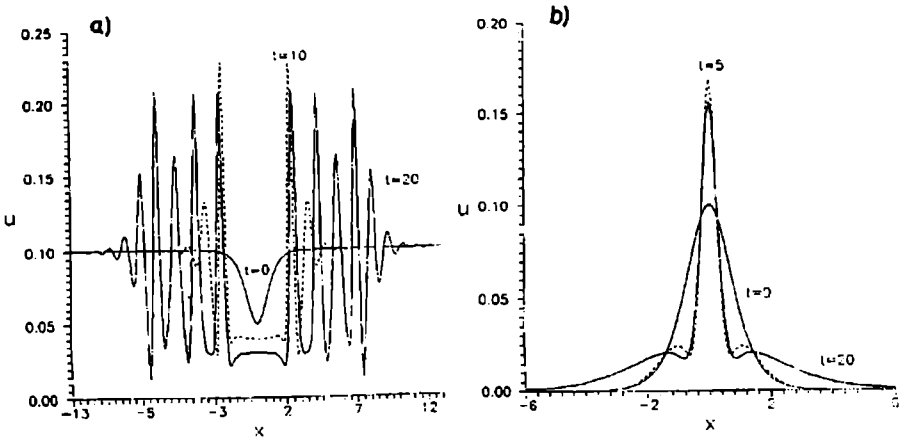


Fig. 12. Profiles of modulation envelope for the NS equation with $\alpha = -0.004$ and $\beta = -52$. The initial conditions are: (a) $u(x, t=0) = 0.1 - 0.05\text{sech}^2 x$; (b) $u(x, t=0) = 0.1\text{sech}^2 x$. Note dressed bright solitons at $t = 5$ and $t = 20$

Ryc. 12. Obwiednia fali będącej rozwiązaniem nieliniowego równania Schrödingera z $\alpha = -0,004$ i $\beta = -52$. Warunki początkowe to: (a) $u(x, t = 0) = 0,1 - 0,05\text{sech}^2 x$; (b) $u(x, t = 0) = 0,1\text{sech}^2 x$. Zauważ ubrane jasne solitony w chwilach czasu $t = 5$ i $t = 20$

REFERENCES

- [1] Agrawal G. P., *Phys. Rev. Lett.*, **59** (1992) 880.
- [2] Benjamin T. B., *Proc. Roy. Soc. London Ser., A* **328** (1972) 153.
- [3] Enns R. H., Rangnekar S. S., Kaplan A. E., *Phys. Rev.*, **35 C** (1987) 466.
- [4] Hasegawa A., *Optical Lett.*, **9** (1984) 288.
- [5] Hasegawa A., *Optical Solitons in Fibers, Springer Tracts in Modern Physics*, 116, Springer-Verlag, Berlin 1989.
- [6] Hasegawa A., Tappert F., *Appl. Phys. Lett.*, **23** (1973) 171.
- [7] Holm D. D., Marsden J. E., Ratiu T., Weinstein A., *Phys. Rep.*, **123** (1985) 1.
- [8] Infeld E., Rowlands G. Z., *Z. Physik B* **37** (1980) 277.
- [9] Infeld E., Rowlands G. Z., *Nonlinear Waves, Solitons and Chaos*, Cambridge Univ. Press, Cambridge 1990.
- [10] Laedke E. W., Spatschek K. H., [in:] *Differential Geometry, Calculus of Variations, and Their Applications*, G. M. Rassias and Th. M. Rassias (eds.), Marcel Dekker Inc., New York 1985.
- [11] Marsden J. E., (1984) *Hamiltonian Structures and Stability*, Lecture Notes by G. Schwartz, Lectures given at Clausthal-Zellerfeld, July 16–20.
- [12] Menyuk C. R., *J. Opt. Soc. Am.*, **B 5** (1988) 399.
- [13] Murawski K., *Acta. Phys. Polon.*, **A 80** (1991a) 485.
- [14] Murawski K., *Acta. Phys. Polon.*, **A 80** (1991b) 495.
- [15] Murawski K., *Ann. Physik.*, **1** (1992) 236.
- [16] Murawski K., Edwin P. M., *J. Plasma Phys.*, **47** (1992) 75.

- [17] Murawski K., Koper R., *Ann. UMCS Sec. AAA*, XLVI/XLVII (1991/1992) 317–327.
- [18] Murawski K., Storer R., *Wave Motion* 41 (1989) 309.
- [19] Murawski K., Ziemkiewicz J., Infeld E., *Wave Motion* 13 (1991) 337.
- [20] Parkes E. J., *J. Phys. A: Math. Gen.*, 21 (1988) 2533.
- [21] Tomlinson W. J., Hawkins R. J., Weiner A. M., Heritage J. P., Thurston R. N., *J. Opt. Soc. Am.*, B 6 (1989) 329.
- [22] Wai P. K., Menyuk C. R., Lee Y. C., Chen H. H., *Opt. Lett.*, 11 (1987) 464.
- [23] Watanabe S., Yoshimura K., *J. Phys. Soc. Japan* 58 (1989) 821.
- [24] Zhelyazkov I., Murawski K., 1993, *J. Plasma Phys.*, submitted.

STRESZCZENIE

Nieliniowa stabilność fal będących rozwiązaniem nieliniowego równania Schrödingera analizowana jest przy pomocy teorii Liapunowa i przybliżenia numerycznego. Przybliżenie numeryczne oparte jest na metodzie szybkich transformat Fouriera (użytych do obliczania pochodnych przestrzennych) i metodzie *skoku zaby* użytej do reprezentacji pochodnej czasowej. W artykule wykazano, że jasne i ciemne solitony są stabilne ze względu na szeroki zakres zaburzeń. Stabilność fal okresowych analizowana jest także w tym celu, by pokazać przykład fali niestabilnej. Wyniki te są w zgodzie z przewidywaniami liniowych teorii stabilności fal. Symulacje numeryczne pokazują transformacje impulsów w sekwencji solitonów jasnych i ciemnych.